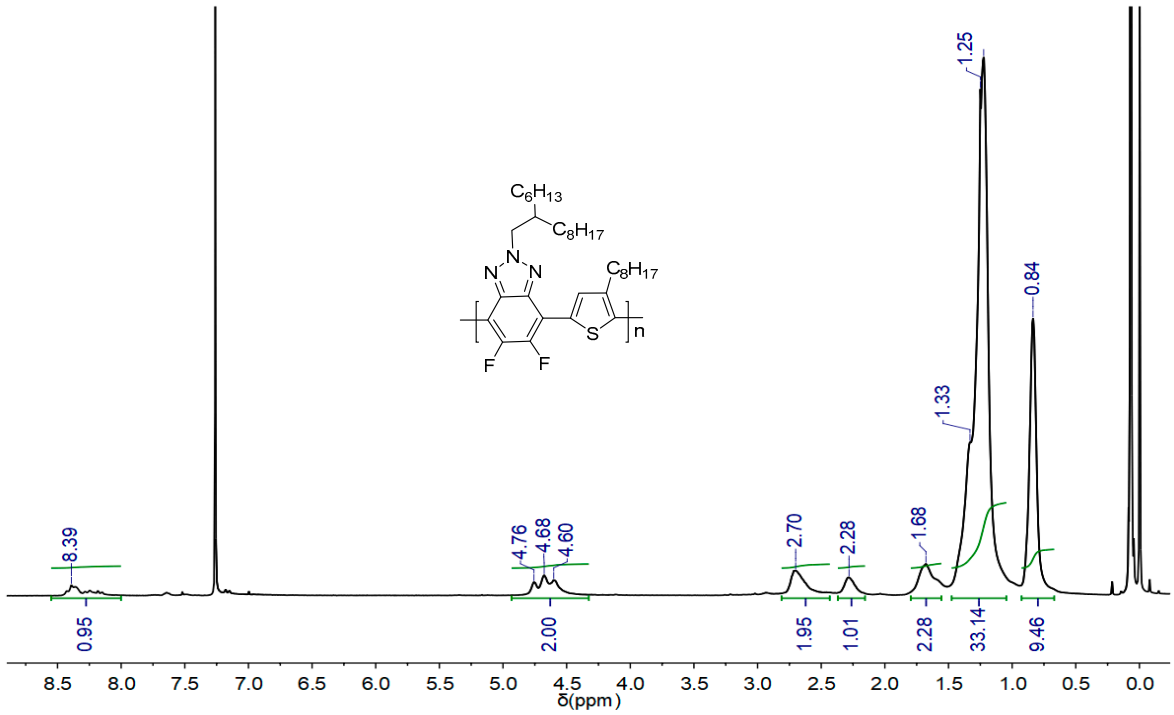

Figure S1. ^{1}H NMR spectrum of **P1** in $CDCl_3$.

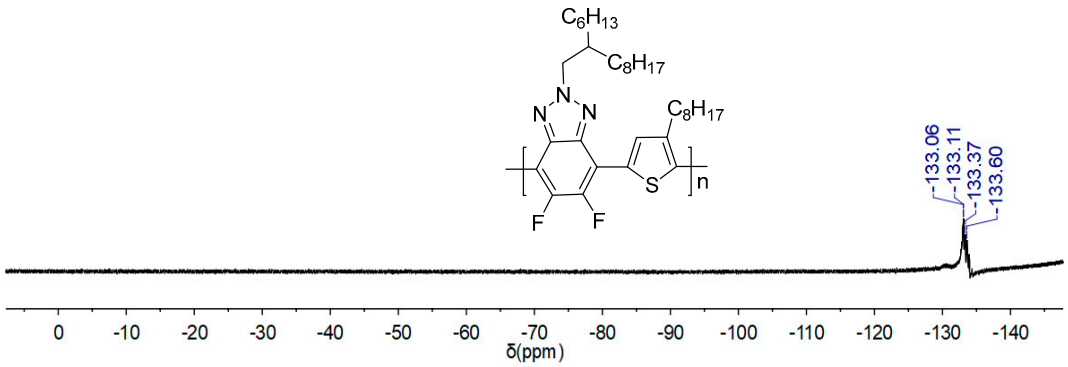

Figure S2. ^{19}F NMR spectrum of **P1** in $CDCl_3$.

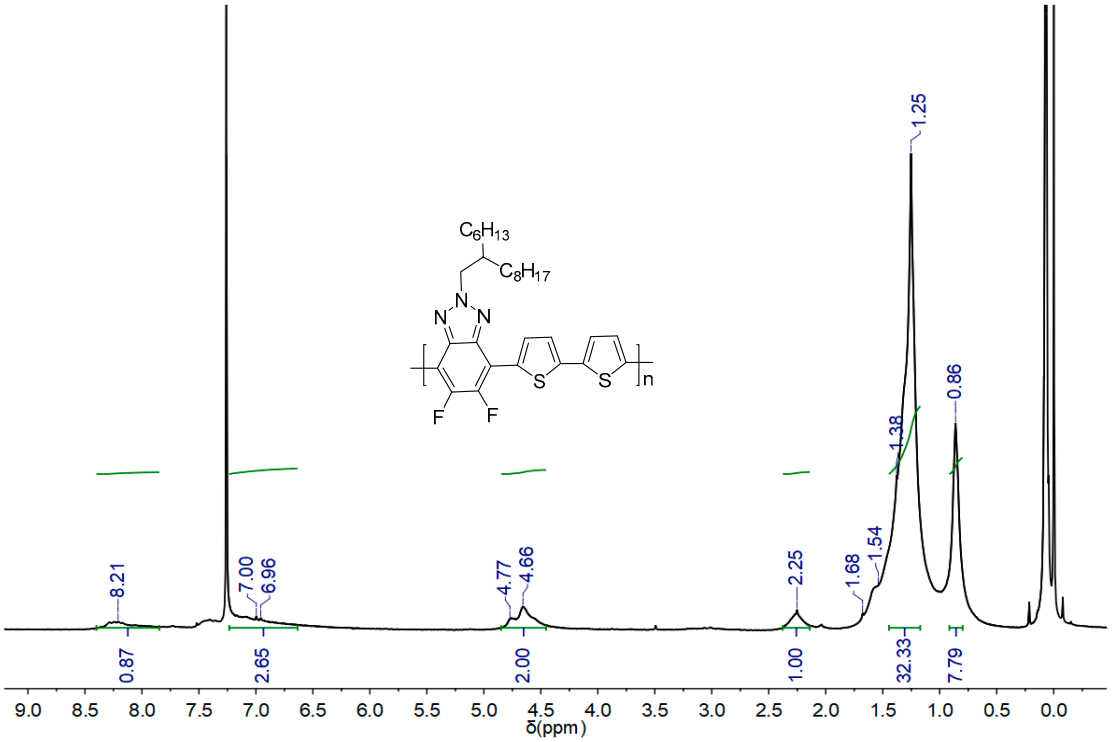

Figure S3. ^{1}H NMR spectrum of **P2** in $CDCl_3$.

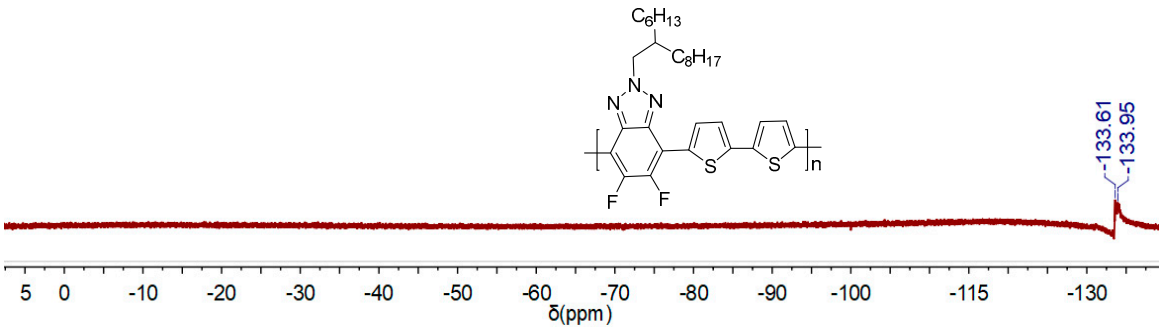

Figure S4. ^{19}F NMR spectrum of **P2** in $CDCl_3$.

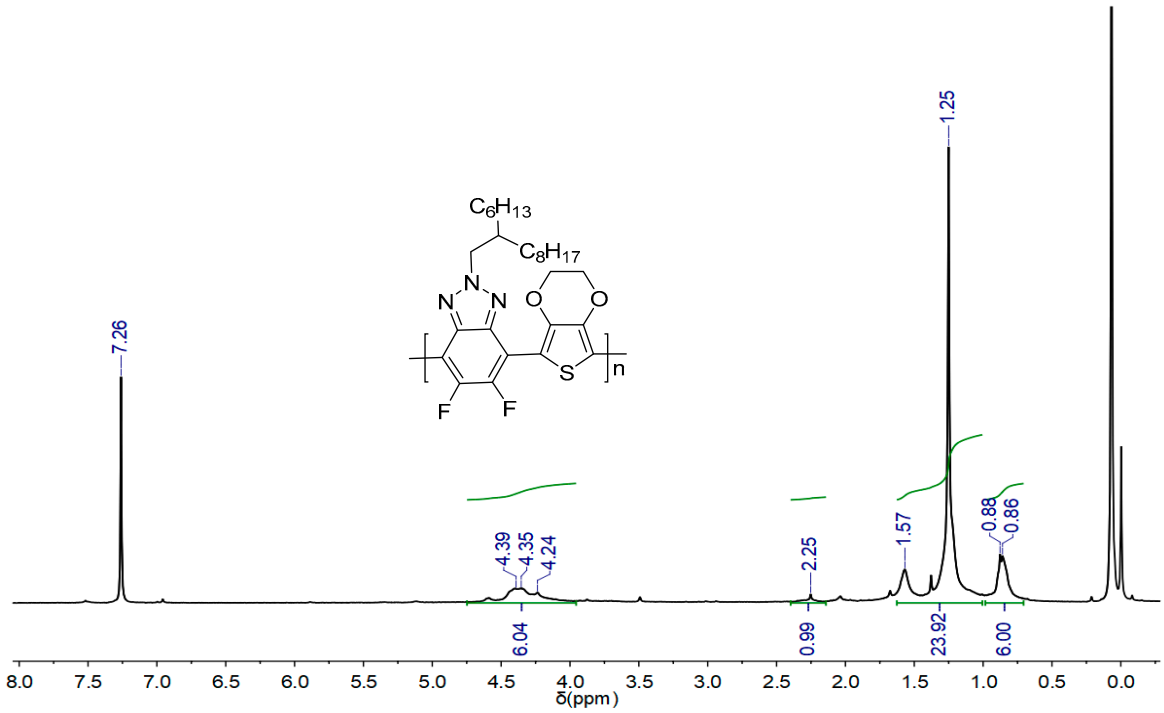

Figure S5. ^{1}H NMR spectrum of **P3** in $CDCl_3$.

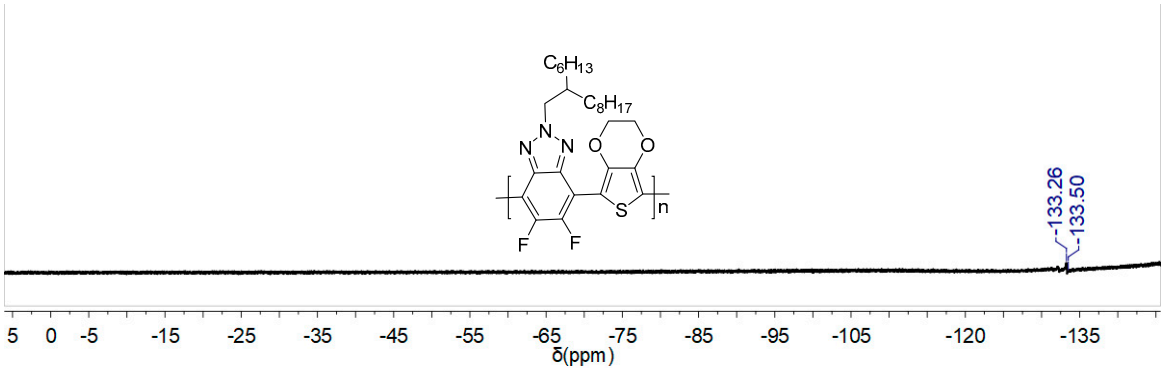

Figure S6. ^{19}F NMR spectrum of **P3** in $CDCl_3$.

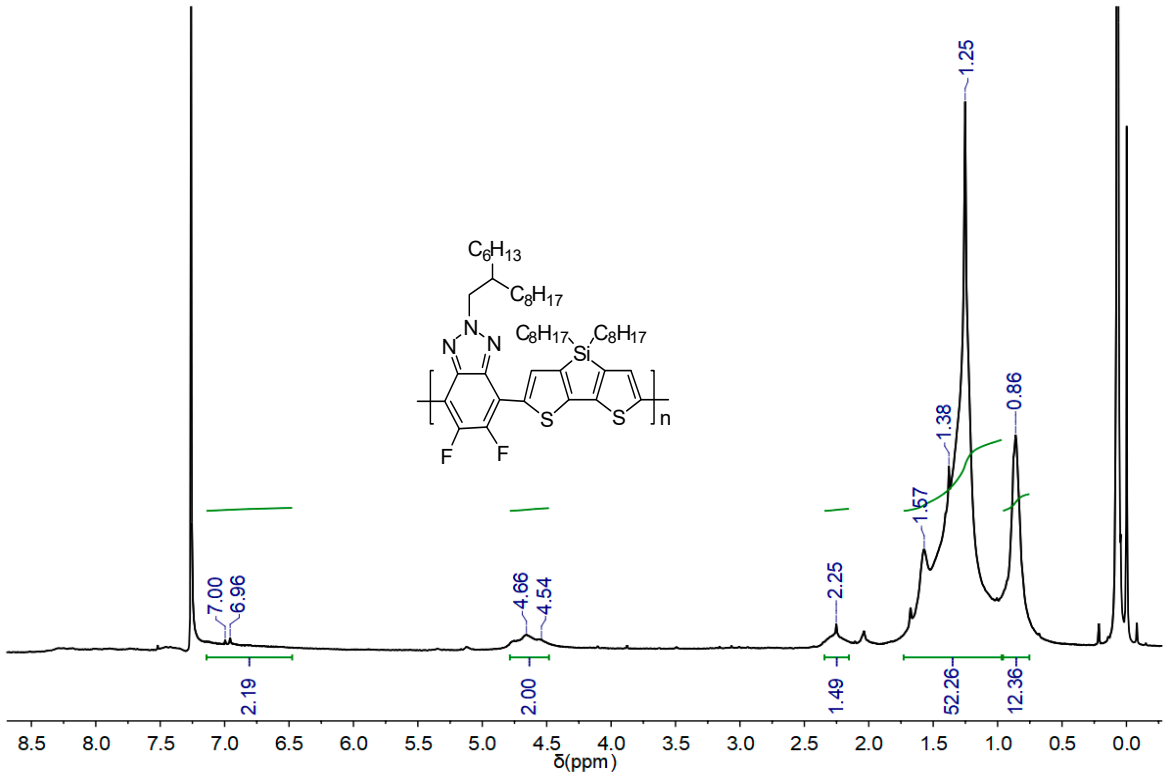

Figure S7. ^{1}H NMR spectrum of **P4** in $CDCl_3$.

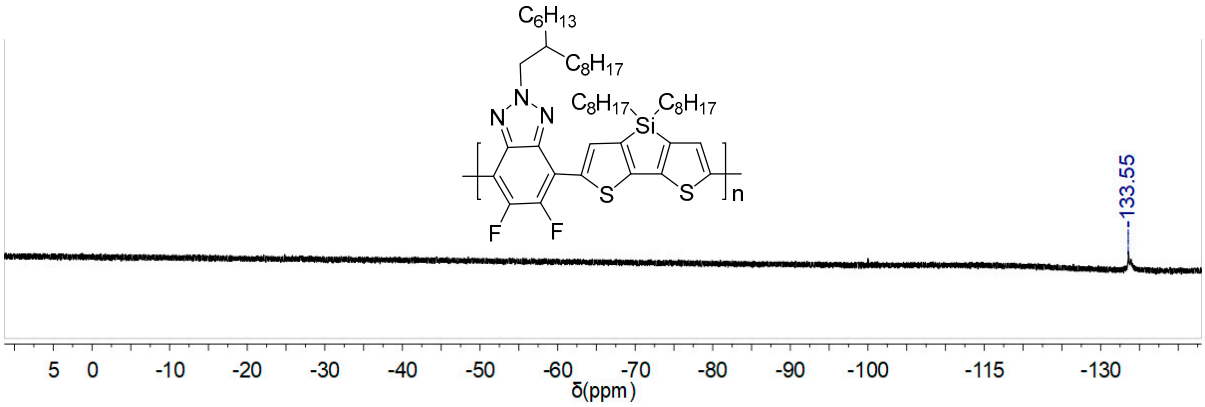

Figure S8. ^{19}F NMR spectrum of **P4** in $CDCl_3$.

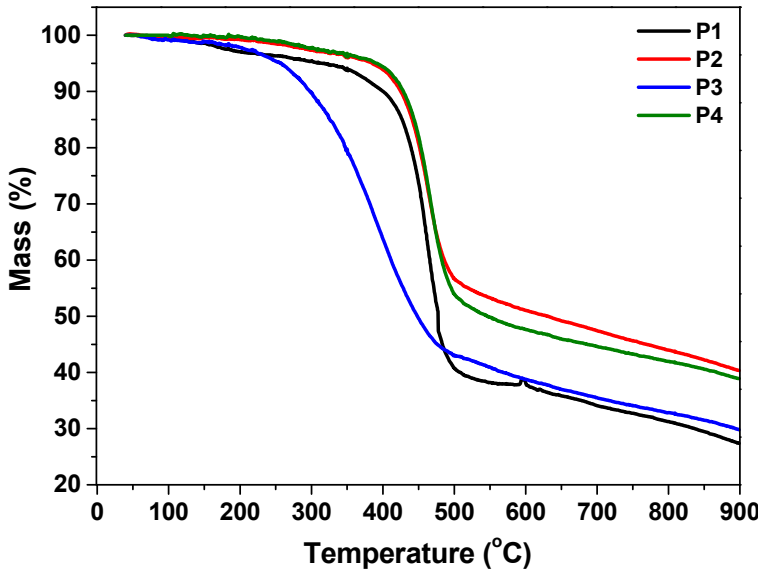

Figure S9. TGA curves of **P1-P4.** The heating rate is 10 °C·min^{-1} under pure nitrogen.

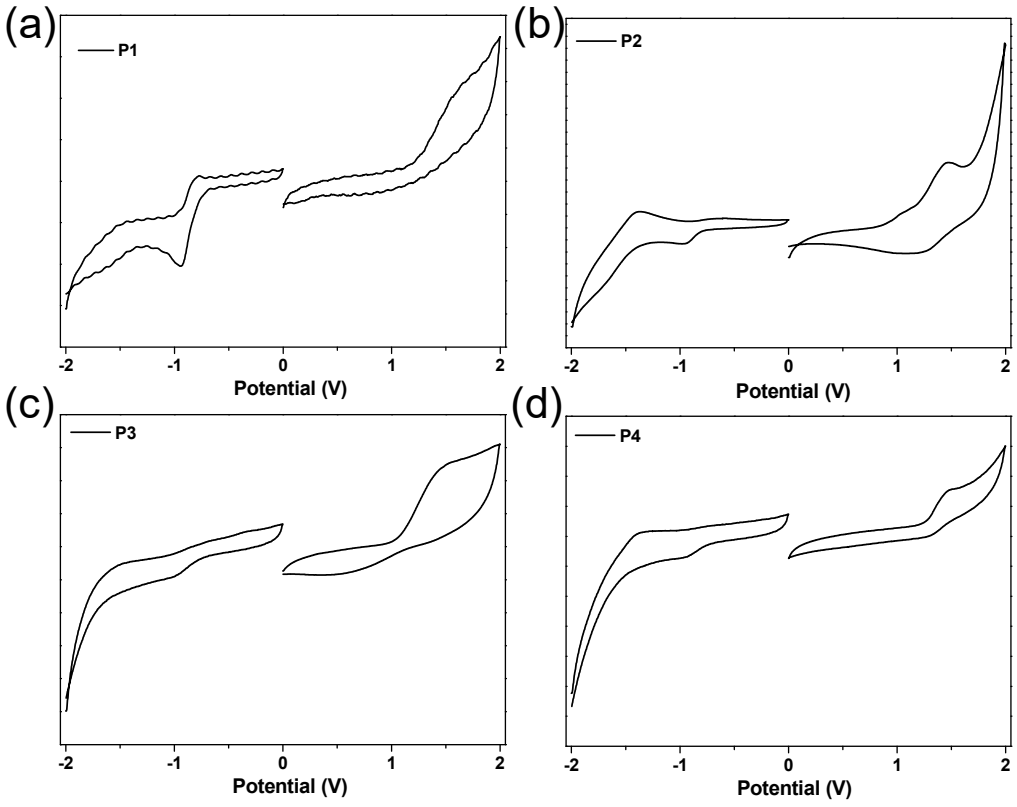

Figure S10. Cyclic voltammograms of **P1-P4** films on a glassy carbon electrode measured in 0.1 M of Bu_4NPF_6 acetonitrile solutions at a scan rate of 100 mV s^{-1}.

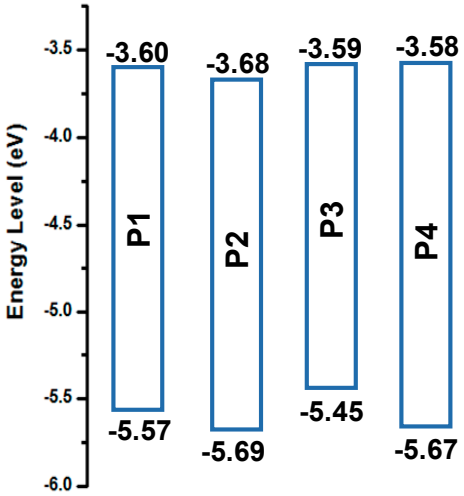

Figure S11. Schematic energy-level diagrams of **P1**-**P4.** Energy levels are estimated from the cyclic voltammetry (Figure S10). E_{HOMO} = -(4.8 + E_{onset}^{ox} – $E_{Fc/Fc+}^{ox}$) eV; E_{LUMO} = -(4.8 + E_{onset}^{red} – $E_{Fc/Fc+}^{red}$) eV. E_g^{cv} = E_{HOMO} - E_{LUMO}.

.

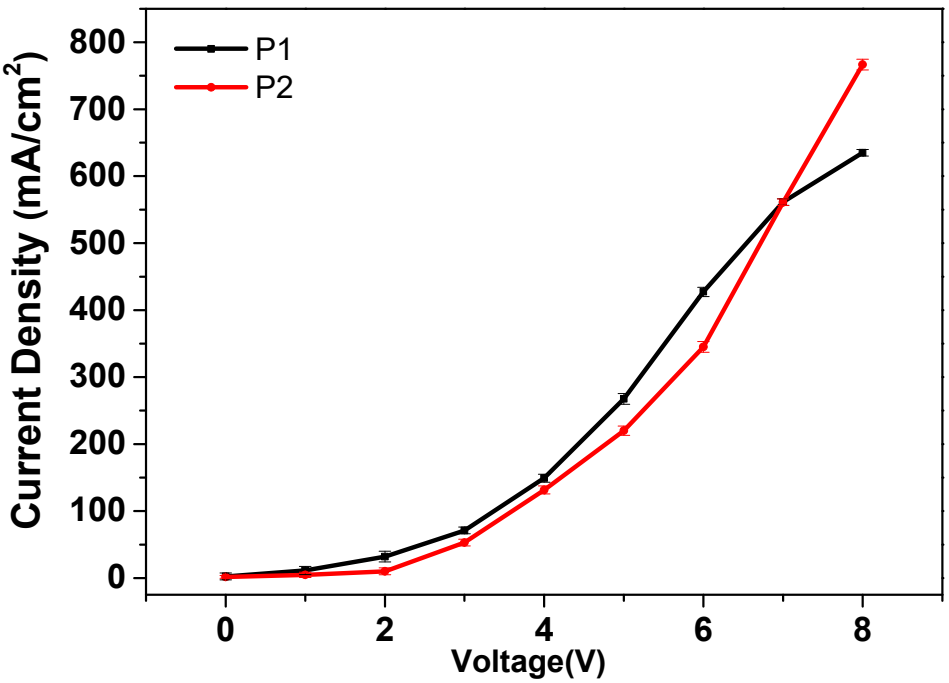

Figure S12. The current density-voltage curve of **P1** and **P2**-based devices.